Title page

Two dimensional temperature measurement characteristics in pulverized coal combustion field by computed tomography-tunable diode laser absorption spectroscopy

Zhenzhen Wang[1,2], Takahiro Kamimoto[2], Yoshihiro Deguchi[2,1,*], Wangzheng Zhou[1],

Junjie Yan[1,2], Kazuki Tainaka[3], Kenji Tanno[3], Hiroaki Watanabe[4], Ryoichi Kurose[5]

[1]State Key Laboratory of Multiphase Flow in Power Engineering, Xi'an Jiaotong University, Xi'an 710049, China

[2]Graduate School of Advanced Technology and Science, Tokushima University, Tokushima 770-8501, Japan

[3]Central Research Institute of Electric Power Industry, Kanagawa, 240-0196, Japan

[4]Kyushu University, Fukuoka, 819-0395, Japan

[5]Kyoto University, Kyoto, 615-8540, Japan

Corresponding author: Yoshihiro Deguchi

Graduate School of Advanced Technology and Science, Tokushima University

TEL: (+81)-88-656-7375

FAX: (+81)-88-656-9082

Email address:ydeguchi@tokushima-u.ac.jp

Postal address: 2-1, Minamijyosanjima, Tokushima 770-8506 Japan

Abstract

Two dimensional temperature and concentration distributions are important parameters for pulverized coal combustion used for power plant to understand the combustion field and develop the high efficient combustion technologies. However, it is difficult to measure two dimensional temperature and concentration in pulverized coal combustion field using conventional measurement technologies because pulverized coal combustion produces lots of dust and strong emission from its frame. This paper focused on the application of two dimensional temperature distribution measurement method based on the combination of computed tomography and tunable diode laser absorption spectroscopy using absorption spectra of water vapor at 1388nm and 1343nm, which show the better characteristics of spatial-temporal resolution, fast response, high sensitivity, self-calibration and optical accessibility compared with thermocouples and other laser diagnostics. Accuracy of temperature measurement using tunable diode laser absorption spectroscopy was improved by applying the corrected spectroscopic database. Computed tomography reconstruction accuracy of 16 laser-paths configuration was evaluated, which presented the consistent temperature between assumed and reconstructed distributions. This computed tomography-tunable diode laser absorption spectroscopy was successfully applied to pulverized coal flame for two dimensional temperature measurement with 1 ms temporal resolution for time-series two dimensional temperature measurement. The pulverized coal flame temperature distribution was compared to Methane-Air flame to demonstrate its feasibility and rationality due to the main heat release produced by methane fuel. It is verified the applicability to various types of combustor, especially the pulverized coal combustion field. It will be benefit for optimal operation control and combustion efficiency improvement by combustion organization or new design of combustion system.

1. Introduction

Pulverized coal combustions are mainly used for power plant in electric industries. The improvement of combustion efficiency and reduction of pollutants such as NOx, SOx and particles are important for energy conservation and emission reduction in industry, as well as for human lives and science development. Therefore, it requires the advanced measurement technologies in pulverized coal combustion to control the important combustion parameters such as temperature and species concentrations for combustion organization and new design of combustion system [1,2]. Conventionally a thermocouple and a sampling probe have been widely used as a temperature and concentration measurement devices. However, it is intrinsically a point measurement method and difficult to precisely measure temperature and concentration distributions in pulverized coal combustion. In past decades, laser-based measurement technologies have been applied for measurements of combustion phenomena [3,4].

Recently, many studies related to temperature and species concentration measurements in combustors using tunable diode laser absorption spectroscopy (TDLAS) have been reported as a non-contact temperature and species concentration measurement technique with high sensitivity and fast response [5-9], such as exhaust gas, different engines, coal gasifier and so on, under various conditions. The TDLAS technique gives self-calibration to reduce the noise effect such as particles and dusts because the laser wavelength is rapidly modulated at kHz rates. With the development of computed tomography (CT), tomography technique has been utilized in absorption spectroscopy [10-14]. Two dimensional (2D) temperature and concentration distributions can be obtained by combining CT with TDLAS. A robust, spatially scanning, open-path TDLAS hygrometer was developed using retro-reflective foils for fast tomographic 2D water vapor concentration field measurement [15]. The axisymmetric temperature and gas concentration distributions were reconstructed by combining fan-beam TDLAS with onion-peeling deconvolution [16]. The 2D temperature distribution was reconstructed using H_2O absorption spectroscopy [17-20]. The simultaneous tomographic reconstructions of temperature and species concentration have been

numerically investigated [21,22]. The 2D temperature and various species concentration distributions were also studied using computed tomography-tunable diode laser absorption spectroscopy (CT-TDLAS) [23-27]. Compared to the point measurement, the combustion field can be evaluated in more detail by measuring 2D temperature and concentration distributions. However, its application to flames with dust and strong flame emission such as coal combustion still remains to be one of the major challenges for CT-TDLAS. It is also one of the common problems for laser diagnostics. The particle, dust and flame emission become a problem for quantitative analyses [3].

This paper focused on 2D temperature detection characteristics of pulverized coal flames using the combination of TDLAS and CT reconstruction (CT-TDLAS), in which TDLAS can eliminate the effect of dust and flame emission by the self-calibration for each laser scanning using direct absorption spectroscopy. Theoretical H_2O absorption spectra at 1388 nm and 1343 nm calculated by a revised HITRAN database (high-resolution transmission molecular absorption database) were used for temperature measurement to enhance its accuracy. H_2O absorption spectra at 1343 nm with high sensitivity of temperature measurement in 1000-2000K was selected to maintain the accuracy of measurement results. The verification tests were also performed in a Methane-Air premixed flame using CT-TDLAS based on the spectroscopic water vapor absorption data. The temperature measurement results of pulverized coal flame demonstrate for the first time that CT-TDLAS was successfully applied to pulverized coal combustion field and it shows a potential to be applicable to the analysis of pulverized coal combustion.

2. Theory

Principle of TDLAS is based on Lambert Beer's law. When a laser beam passes through the measurement area containing target gases, the intensity of transmission is related to the absorber concentration according to this law [3]:

$$I_\lambda/I_{\lambda 0} = exp\{-A_\lambda\} = exp\left\{-\sum_i n_i L \sum_j S_{i,j}(T)G_{Vi,j}(n_i,T,P)\right\} \quad (1)$$

Here, $I_{\lambda 0}$ is the incident light intensity, I_λ is the transmitted light intensity, A_λ is the absorbance, n_i is the number density of species i, L is the path length, $S_{i,j}$ is the temperature dependent absorption line intensity of the absorption line j, and $G_{Vi,j}$ is the line broadening function which depends on temperature T, pressure P and co-existing species concentrations. One of the merits of TDLAS is its high response by continuously scanning laser wavelengths at the rate higher than kHz, which gives self-calibration to reduce noise effect caused by particles and dusts. Theoretical H_2O absorption spectra in near-infrared region can be calculated by the HITRAN database [28]. Four absorption lines located at 1388.135 nm (#1), 1388.326 nm (#2), 1388.454 nm (#3) and 1343.298 nm (#4) with remarkable temperature dependence were chosen for temperature measurement. The line at 1343.298 nm (#4) is one of the stronger H_2O absorption lines in high temperature conditions (1000-2000K). The specifically theoretical H_2O absorption spectra and the temperature dependence were presented elsewhere [18]. One of the great features of TDLAS is that the attenuation of laser beam and flame emission can be corrected by measuring the scanning laser intensity [3]. It is often called self-calibration of TDLAS. Utilizing this feature, the quantitative results of temperature and concentration can be measured in the condition with dust and flame emission.

When several laser beams are transmitted across the measurement area containing the target gases, integrated absorbance of each laser path is related to the absorber temperature and concentration distributions along the path as in the following formula [18,19]:

$$A_{\lambda,p} = \sum_q n_{p,q} L_{p,q} \alpha_{\lambda,p,q} = \sum_q n_{p,q} L_{p,q} S_\lambda(T_{p,q}) G_{V,\lambda}(n_{p,q}, T_{p,q}, P) \quad (2)$$

Here, $A_{\lambda,p}$ is integrated absorbance of some wavelength λ in a path p, $n_{p,q}$ is the species

number density in a path p inside a position q, $\alpha_{\lambda,p,q}$ is absorption coefficient of some wavelength λ inside a position q on the path depending on temperature and species concentration, $L_{p,q}$ is path length inside the position q. Using a set of equation (2), 2D distributions of concentration and temperature are reconstructed by CT. Sets of H_2O concentrations and temperatures at analysis positions are obtained by the best-fitted distributions for a given measurement of $A_{\lambda,p}$ using the minimization procedure shown in **Figure 1**. The 2D temperature and concentration distributions can be defined to employ the 2D polynomials as presented in Equations (3) and (4). 2D temperature and concentration information is used to calculate the absorption coefficient at each point to improve the accuracy and flexibility.

$$T(x,y) = \sum_{k=0}^{m} \sum_{l=0}^{k} b_{k-l,l} x^{k-l} y^l = F_T(b_{k,l})$$

(3)

$$n(x,y) = \sum_{k=0}^{m} \sum_{l=0}^{k} a_{k-l,l} x^{k-l} y^l = F_n(a_{k,l})$$

(4)

Here, x and y are the axes of the measurement area, a and b are the polynomial parameters. m is the polynomial order, which is determined by the number of laser paths and the laser path configuration. m is usually chosen as 8-10 for $p=16$, 10-14 for $p=32$, and 14-18 for $p=64$. In this study m was chosen as 10 and q was 40. 460 wavelength measurement points were detected during the wavelength scanning. Equation (2) consisted of 7360 equations and there were 132 unknown factors including 66 $a_{k,l}$ and 66 $b_{k,l}$.

Temperature and species concentration at each analysis point are determined using a multifunction minimization method to minimize the spectral fitting error between theory and experiment.

$$Error = \sum_{\lambda,p} \left\{ (A_{\lambda,p})_{theory} - (A_{\lambda,p})_{experiment} \right\}^2$$

(5)

$$A_{\lambda,p} = \sum_q n_{p,q}\alpha_{\lambda,p,q}L_{p,q} = n_{p,1}\alpha_{\lambda,p,1}L_{p,1} + n_{p,2}\alpha_{\lambda,p,2}L_{p,2} + n_{p,3}\alpha_{\lambda,p,3}L_{p,3} + \cdots + n_{p,q}\alpha_{\lambda,p,q}L_{p,q} = -\ln\left(\frac{I_{\lambda,p}}{I_{\lambda 0,p}}\right)$$
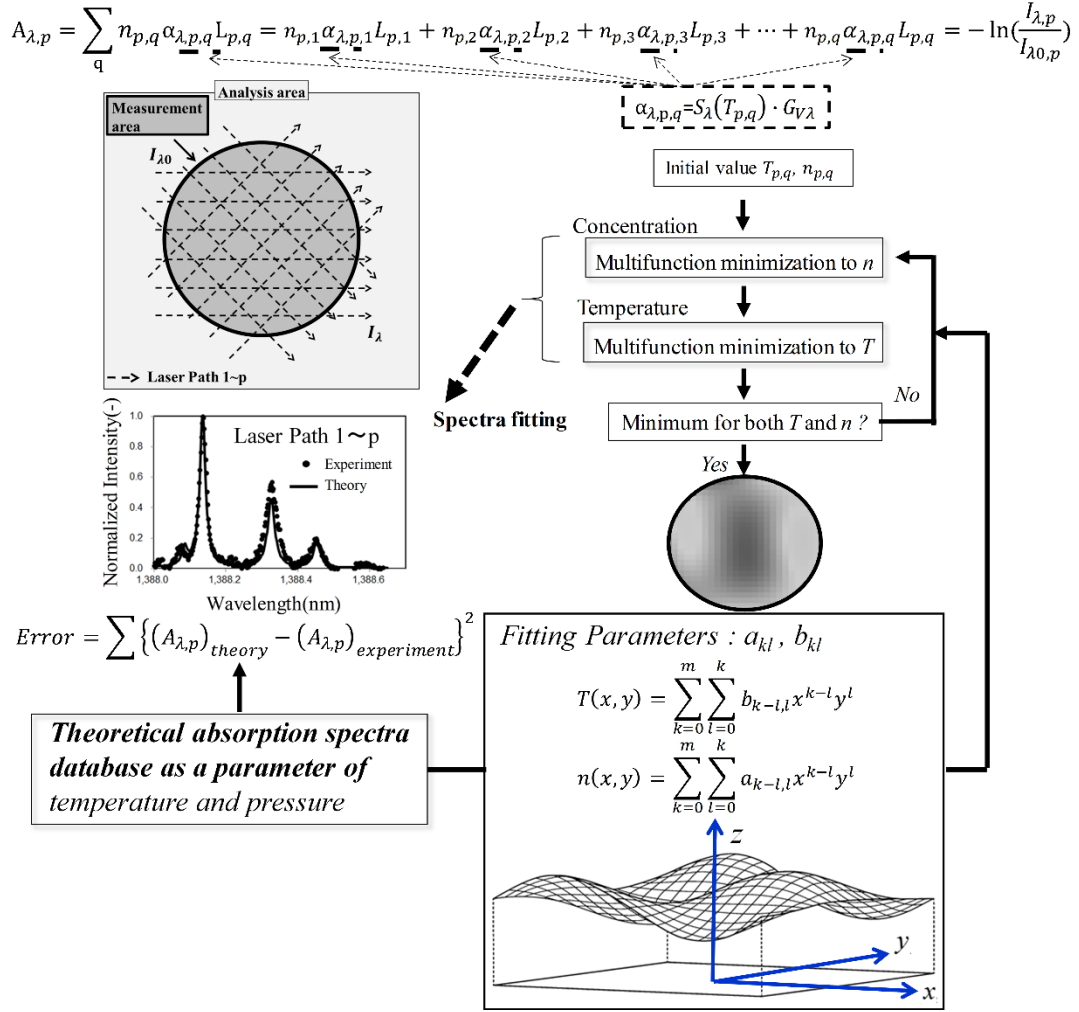
Figure 1 CT configration with laser path and CT algorithm.

The measurement error depends on some factors such as number of beams [17,23,25], view angles [14,16], CT-algorism [11,20,21], uncertainty of spectral database [18,19] and others [15,24,26,27]. The downhill simplex and Levenberg-Marquardt methods for multifunction minimization were used in this study. One of the most prominent merits of this method is its stability of reconstruction especially at the edge of measurement area where the laser path number is usually small compared to the center area. This is because the spatial resolution of temperature and concentration distributions is determined by the polynomial order and is not determined locally.

3. Experimental Setup

3.1. Evaluation of temperature measurement accuracy

The temperature measurement accuracy was evaluated by the comparison of TDLAS

and thermocouple. Measurements of H_2O absorption spectra (#1:1388.135nm, #2:1388.326nm, #3:1388.454nm) from 300K to 800K using TDLAS were conducted in a measurement cell with heating furnace as shown in **Figure 2(a)**. Measurements of H_2O absorption spectra (#1:1388.135nm, #2:1388.326nm, #3:1388.454nm, #4:1343.298nm) from 1000K to 2000K using TDLAS were conducted in a flat flame-type burner as shown in **Figure 2(b)**. The measured H_2O absorption spectra were applied to revise the spectroscopic database to improve TDLAS accuracy of temperature measurement. Two distributed feedback (DFB) diode lasers near 1388nm and 1343nm (NTT Electronics Co., NLK1E5GAAA/NLK1S5GAAA) were used to obtain H_2O absorption spectra. The lasers were driven by a diode laser controller (Thorlabs Co., TXP5004) with current source and temperature-control unit (Thorlabs Co., ITC5052). Wavelength scanning was consisted of 5kHz sawtooth ramp using direct absorption spectroscopy, which has better wavelength linearity for spectral evaluation than sinusoidal modulation, with a function generator (Wavefactory Co., WF1946).
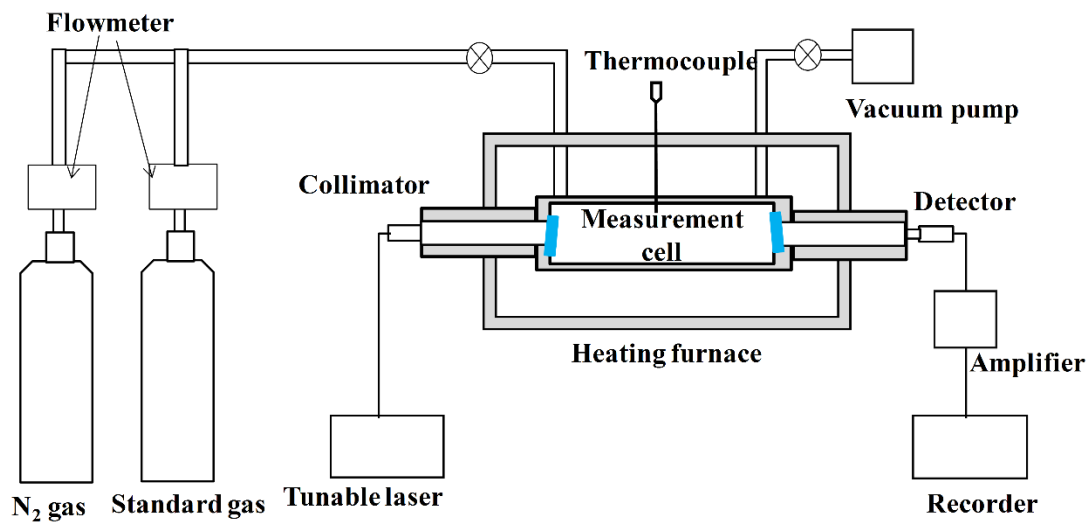
(a) Measurement cell for low temperature range
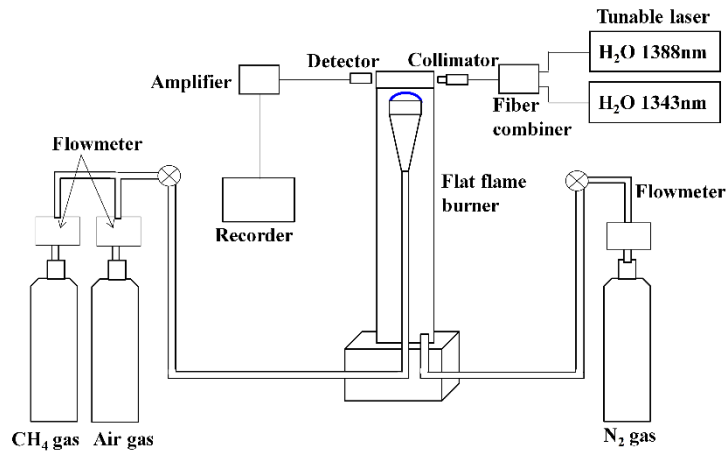
(b) Flat flame burner for high temperature range

Figure 2 Experimental apparatus for evaluation of temperature measurement accuracy.

The DFB laser near 1388nm was utilized in **Figure 2(a)** for the low temperature range measurement from 300K to 800K. The laser beam irradiated into the measurement cell using a collimator (THORLABS Co., 50-1310-APC). The transmitted light was detected by a photodiode (Hamamatsu Photonics and G8370-01) and amplified by an amplifier (Stanford Research Systems, SR445A). The amplified signal was directly stored by a recorder (HIOKI E.E. Co., 8861 Memory High coda HD Analog16). The temperature in the measurement cell was controlled by the heating furnace.

For the high temperature range measurement from 1000K to 2000K in **Figure 2(b)**, these two DFB lasers were scanned at 5kHz and the laser outputs were mixed using a fiber combiner as one laser beam. The laser beam passed through the flat flame-type burner using the collimator. The transmitted laser intensity was also detected by the photodiode. The photodetector signal was amplified by the amplifier and directly stored by the recorder. The flat flame-type burner had the double tube structure composed of a sintered bronze filter and an external pipe. Methane (CH_4) used as a fuel was mixed with air and supplied through the sintered bronze filter with a diameter of 45mm. CH_4 and air flow rates through nozzle were $1.6 \times 10^{-5} \sim 2.7 \lozenge 10^{-5}$ (m^3/s, ntp) and $16 \times 10^{-5} \sim 27 \times 10^{-5}$ (m^3/s, ntp), respectively. Flame temperature was controlled by changing those flow rates and a number of meshes which were set above the sintered bronze filter. In each case, the air-to-fuel ratio was 0.95.

3.2. 2D temperature measurement in pulverized coal combustion using CT-TDLAS

Figure 3 shows the CT-TDLAS experimental setup for a pulverized coal burner. The burner had triplex tube structure composed of internal nozzle, external pipe and outer pipe. The pulverized coal was introduced into the system by a feeder (Nisshin Engineering, Feedcon-μ Mtype). The feed rate of pulverized coal was $1.4×10^{-2}$ g/s. Pulverized coal was mixed with air and supplied through the internal nozzle with a diameter of 6mm using an ejector (Fukuhara, M-05). CH_4 was supplied through the external pipe with a diameter of 10mm. Ambient air was also supplied through the outer pipe with a diameter of 65mm. The 16-path CT-TDLAS measurement cell (Smart Laser & Plasma Systems Co., CT-TDLAS-16LP-HTPC-R70) was set at the position of 54mm above the burner. The inner diameter of 16-path CT-TDLAS measurement cell was 70mm. 2D temperature measurements in the CH_4-Air flame and pulverized coal flame were performed using the burner with the 16-path CT-TDLAS cell. 2D temperature distribution in CH_4-Air flame was also measured by a platinum-platinum rhodium thermocouple with a diameter of 100μm (ANBE SMT Co., BM-100 -100 -050), which was compared to 2D temperature result detected by the 16-path CT-TDLAS cell to verify the consistency of temperature measurement results. The experimental parameters for the burner combustion are summarized in **Table 1**.
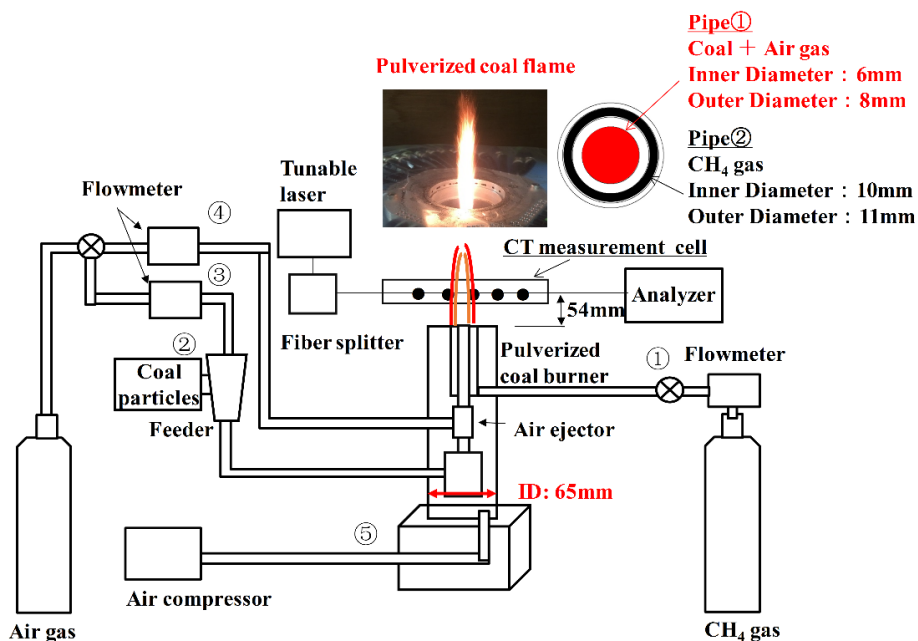
(a) CT-TDLAS experimental setup for a pulverized coal burner
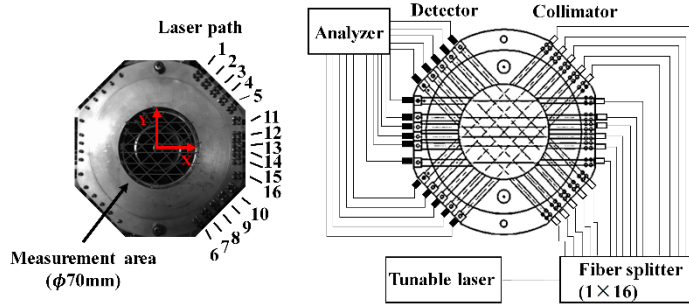
(b) 16-path CT-TDLAS measurement cell

Figure 3 Experimental system for 2D temperature measurement in a pulverized coal burner using CT-TDLAS.

Table 1 Experimental parameters for burner combustion.

	①CH$_4$ (10^{-5} m^3/s)	②Coal (10^{-2} g/s)	③Feeder dry air/ Mixed air (10^{-5} m^3/s)	④Air (10^{-5} m^3/s)	⑤Ambient air by compressor (10^{-5} m^3/s)
Pulverized coal flame	5	1.4	4.8	45	133
CH$_4$-Air flame	0.58	0	3.3	0	133

Figure 3(b) shows the schematic diagram of 16-path CT-TDLAS measurement cell. CT reconstruction accuracy depends on the number of laser beam, laser beam angles and its geometrical configuration. The geometrical laser beam arrangement was determined to maintain the combustion phenomena with a main reaction field at the center of measurement cell. As optical access ports, 16 collimators and 16 detectors were embedded in the 16-path CT-TDLAS measurement cell. Two DFB diode lasers near 1388nm and 1343nm was used to measure 2D temperature. The two wavelength laser beams were mixed using the fiber combiner and the mixed laser beam was separated by an optical fiber splitter (OPNETI CO., SMF-28e 1310 nm SWBC 2×16) to 16 paths. The separated laser beams irradiated into the flame by the 16 collimators. The transmitted laser intensities were detected by the 16 photodiodes after passing through the flame and then recorded by analyzer including amplifier and recorder.

4. Results and Discussion

In order to measure 2D temperature distribution in pulverized coal combustion field using CT-TDLAS, the temperature measurement accuracy of TDLAS and 16-path CT

reconstruction accuracy were evaluated before the pulverized coal combustion measurement.

4.1. Evaluation of temperature measurement accuracy

H_2O absorption spectra (#1:1388.135nm, #2:1388.326nm, #3:1388.454nm, #4:1343.298nm) from 300K to 2000K were measured using the experimental setups shown in **Figure 2**. The spectroscopic database was corrected using these experimental results. For example, when employing the experimental setup in **Figure 2(b)**, the mole fraction of water vapor formed during combustion was calculated according to the air-to-fuel ratio of 0.95. Five different flame temperature cases controlled by changing the CH_4 and air flow rates and a number of meshes were determined and measured, such as average temperature in case 1: 2048K, case 2: 1864K, case 3: 1354K, case 4: 1265K, case 5: 1244K. The 1D temperature distribution was measured using thermocouple along the laser path. **Figure 4** shows the temperature distributions in each temperature case measured by thermocouple, which was moved along the laser path at 2mm intervals. Around the center of flat flame, it was indicated the uniform temperature distribution in each case.
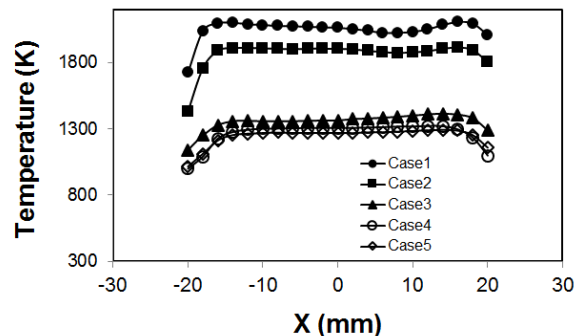
Figure 4 Temperature distribution measured by thermocouple in flat flame burner. (Average temperature in case 1: 2048K, case 2: 1864K, case 3: 1354K, case 4: 1265K, case 5: 1244K).

In these five temperature cases, the temperature was also measured by TDLAS. **Figure 5** shows the theoretical and experimental absorption spectra of water vapor near 1388nm and 1343nm in case 1 with the average temperature of 2048K. The absorption spectra at 1388.0-1388.6nm and 1343.0-1343.5nm present the large differences between TDLAS measured results and theoretically calculated results in **Figure 5(a)**

and **Figure 5(c)**. The theoretical absorption spectra of H_2O were revised using the measured spectral parameters, which include the set of temperature dependent absorption line strength ($S_{i,j}(T)$) in the ranges of 1388.0-1388.6nm and 1343.0-1343.5nm [3,18]. **Figure 5(b)** and **Figure 5(d)** show the theoretical absorption spectra using the corrected spectroscopic database and experimental absorption spectra. The consistency was increased significantly. In this study, the theoretical H_2O absorption spectra from 300K to 2000K were revised according to these experimental results by TDLAS to improve the measurement accuracy.
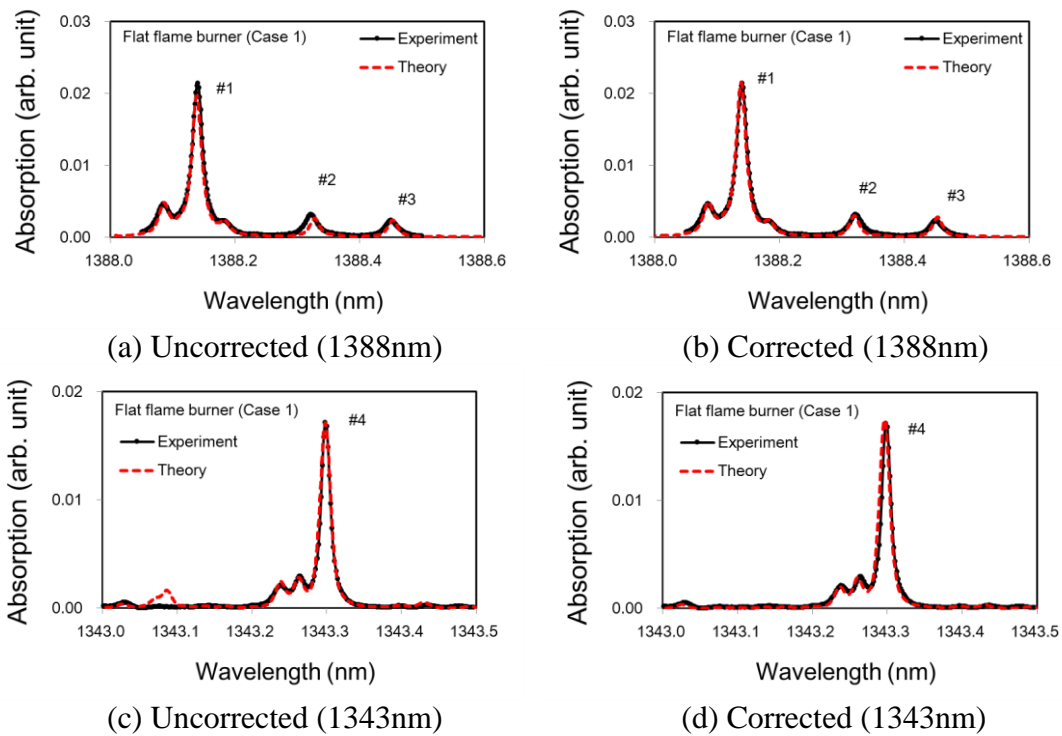
(a) Uncorrected (1388nm)　　　　　(b) Corrected (1388nm)

(c) Uncorrected (1343nm)　　　　　(d) Corrected (1343nm)

Figure 5 Theoretical and experimental absorption spectra of water vapor using uncorrected and corrected spectroscopic database in case 1.

The temperature from 300K to 2000K was measured by TDLAS and thermocouple. The comparison of measured temperature between TDLAS and thermocouple is shown in **Figure 6** under different temperature conditions. The temperature measured by TDLAS was calculated using the uncorrected and corrected spectroscopic database, respectively. The temperature measured by TDLAS using corrected spectroscopic database showed the improved linearity and accuracy compared to the measured temperature by thermocouple with the radiation correction. It is demonstrated that the correction of spectroscopic database has led to better temperature measurement

accuracy for TDLAS technique, which is one essential requirement for 2D temperature measurement by CT-TDLAS.
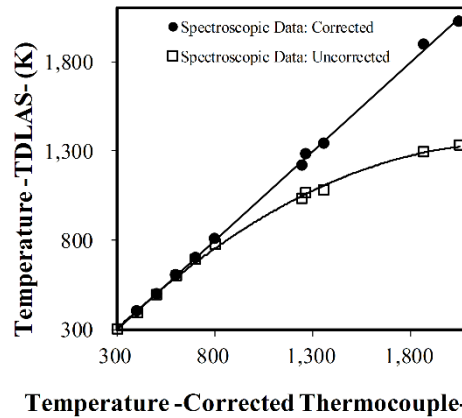
Figure 6 Comparison of measured temperature by TDLAS and thermocouple.

4.2. Evaluation of CT reconstruction accuracy

CT reconstruction is also significant for 2D measurement. The CT algorithm for temperature reconstruction was verified by comparing the assumed temperature distribution and its reconstruction. Two different temperature distribution conditions were assumed in the measurement area of 16-path CT-TDLAS measurement cell, including Condition 1 with flame in center and Condition 2 with shifted flame. The 16 spectra were calculated under the assumed temperature distribution conditions and then the distributions were reconstructed by CT algorithm according to the 16 spectra. **Figure 7** and **Figure 8** shows the comparison of assumed and CT reconstructed temperature distributions in two different conditions.
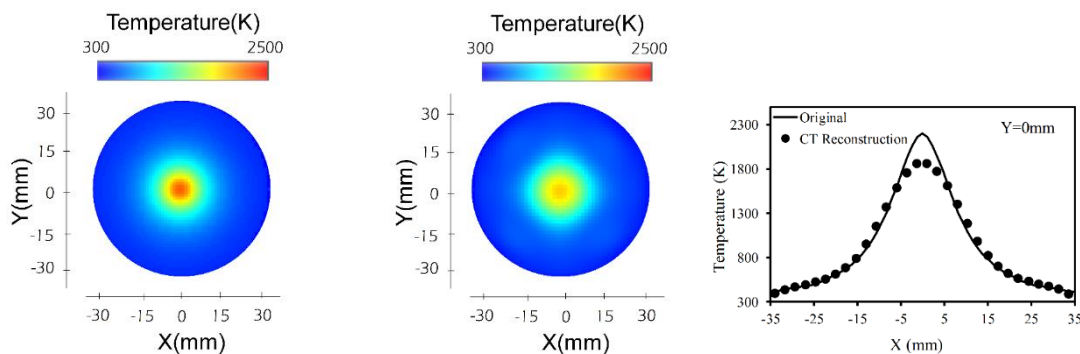
(a)Assumed temperature (b) CT reconstructed temperature (c) Comparison at Y=0mm
Figure 7 Comparison of temperature distributions calculated by 16-path CT-algorithm and assumed temperature in condition 1.
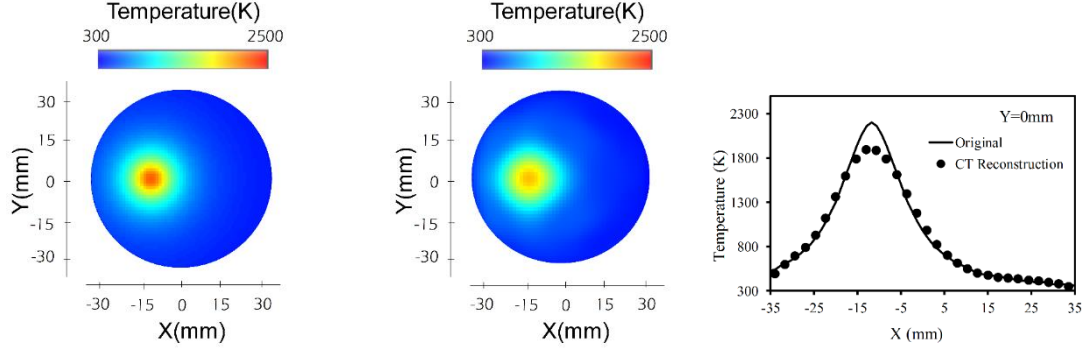
(a)Assumed temperature (b) CT reconstructed temperature (c) Comparison at Y=0mm

Figure 8 Comparison of temperature distributions calculated by 16-path CT-algorithm and assumed temperature in condition 2.

In order to evaluate the accuracy of CT reconstruction quantitatively, the indictors of SSD (sum of squared difference) and ZNCC (zero-mean normalized cross-correlation) were employed. The SSD value has been defined by equation (6). If the SSD value is close to "0", the two profiles have almost same values. The ZNCC value has been defined by equation (7). If this value is close to "1", the two profiles have almost same patterns and the correlation between the two profiles is very high.

$$SSD = \sqrt{\frac{\sum_{i=0}^{N-1}\sum_{j=0}^{M-1}\left\{(T_{i,j})_{virtual} - (T_{i,j})_{CT-TDLAS}\right\}^2}{NM}} \Bigg/ T_R \tag{6}$$

$$ZNCC = \frac{\sum_{i=0}^{N-1}\sum_{j=0}^{M-1}\left\{(T_{i,j} - \bar{T})_{virtual} \times (T_{i,j} - \bar{T})_{CT-TDLAS}\right\}}{\sqrt{\sum_{i=0}^{N-1}\sum_{j=0}^{M-1}(T_{i,j} - \bar{T})_{virtual}^2 \times \sum_{i=0}^{N-1}\sum_{j=0}^{M-1}(T_{i,j} - \bar{T})_{CT-TDLAS}^2}}, \tag{7}$$

$$\bar{T} = \frac{\sum_{i=0}^{N-1}\sum_{j=0}^{M-1}T_{i,j}}{NM}$$

Here, $T_{i,j}$ is the temperature at each point in calculation area, T_R is the representing temperature at 2200K, N is the total number of meshes along the X-axis in the calculation area, and M is the total number of meshes along the Y-axis in the calculation area.

When the flame was in center of Condition 1, **Figure 7(a)** and **Figure 7(b)** show the consistent temperature distribution with the SSD of 0.001 and ZNCC of 0.991. In Condition 2 with shifted flame, SSD and ZNCC were 0.001 and 0.992, which also

illustrated the consistent temperature distribution in **Figure 8(a)** and **Figure 8(b)**. These results were good enough to be considered as almost the same patterns. Therefore, it can be said that the CT reconstructed distributions in the measured area agreed well with the assumed distributions. The CT reconstruction accuracy of laser-path configuration was not affected by flame pattern. The CT reconstructed distribution spread more widely than that of the assumed distribution due to the calculation of CT reconstruction based on limited number of absorbance. **Figure 7(c) and Figure 8(c)** show the comparison of temperature distributions at Y=0mm in two different conditions, which presented the consistent temperature tendency. However, the reconstructed temperature distributions in middle of flame were lower than that of assumed temperature distributions because of the limited laser paths.

4.3. 2D temperature measurement in pulverized coal combustion using CT-TDLAS

Employing the corrected spectroscopic database, 2D temperature measurement was studied by 16-path CT-TDLAS using the experimental setup in **Figure 3**. The gases of CH_4 and air were introduced into the burner to produce the CH_4-Air flame. In order to produce the pulverized coal flame, CH_4 and air gases, as well as pulverized coal, were introduced into the burner for combustion. The burner center was located at the center of 16-path CT-TDLAS measurement cell (X=0mm, Y=0mm). 2D temperature distributions in the CH_4-Air flame and pulverized coal flame were measured by CT-TDLAS based on H_2O absorption spectra (#1:1388.135nm, #2:1388.326nm, #3:1388.454nm, #4:1343.298nm). In the case of CH_4-Air flame, the temperature results measured by thermocouple were detected at interval of 2mm by moving the thermocouple along one laser path at Y=0mm of 16-path CT-TDLAS measurement cell. **Figure 9** shows the comparison of measured temperature distributions at Y=0mm between CT-TDLAS and thermocouple in CH_4-Air flame. The temperature distribution measured by CT-TDLAS shows the consistent tendency with that measured by thermocouple. However, the temperature results of thermocouple were lower than the reconstructed temperature results from measured H_2O absorption spectra, which may be caused by the radiation effects of thermocouple. According to the measurement

results of CH$_4$-Air flame, the feasibility of temperature measurement using CT-TDLAS was verified.
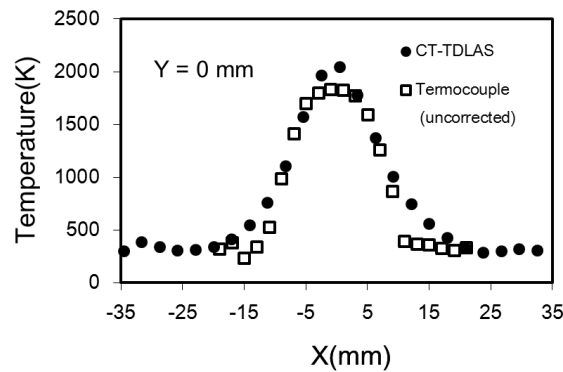
Figure 9 Comparison of temperature distributions at Y=0mm measured by 16-path CT-TDLAS and thermocouple in CH$_4$-Air flame.

2D temperature distributions of CH$_4$-Air flame and pulverized coal flame were reconstructed using CT algorithm. **Figure 10(a)** shows the 2D measurement result of temperature in the CH$_4$-Air flame measured by the 16-path CT-TDLAS cell. When introducing the pulverized coal to the burner, the 2D temperature distribution in the pulverized coal flame was also measured and the measurement result shown in **Figure 10(b)**. As is well-known, the pulverized coal flame showed a strong emission as illustrated in **Figure 3(a)** and it contained the particle and dust including pulverized coal and fly ash. However, the 2D temperature distribution was still successfully reconstructed in the pulverized coal combustion field with particles, dusts and flame emission. Because of its self-calibration feature, the CT-TDLAS measurement result was not affected by the particle, dust and flame emission. Comparing 2D temperature distributions in **Figure 10(a)** and **Figure 10(b)**, the temperature distributions showed the almost same profile and peak temperature between CH$_4$-Air flame and pulverized coal flame. The reason is that the main heat release was produced by fuel of CH$_4$ in these flames.
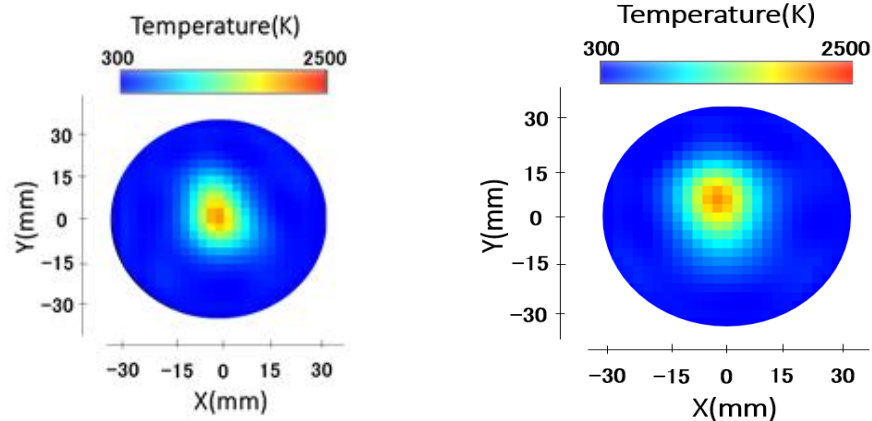
(a) CH₄-Air flame   (b) pulverized coal flame

Figure 10 2D temperature measurement results in CH₄-Air flame and pulverized coal flame using 16-path CT-TDLAS.

This method usually can reach kHz response time depending on applications. Therefore, the dynamic temperature distribution can be detected using CT-TDLAS. **Figure 11** shows the time-series 2D temperature measurement result of the pulverized coal flame. 1 ms temporal resolution was achieved in the pulverized coal combustion field. It is demonstrated from these results that CT-TDLAS is applicable to various flames even if with the particles, dusts and flame emissions for online measurement. The fast 2D temperature measurement becomes possible using the newly developed CT-TDLAS method. The measurement results will provide the basic data for combustion organization and new design of combustion system.
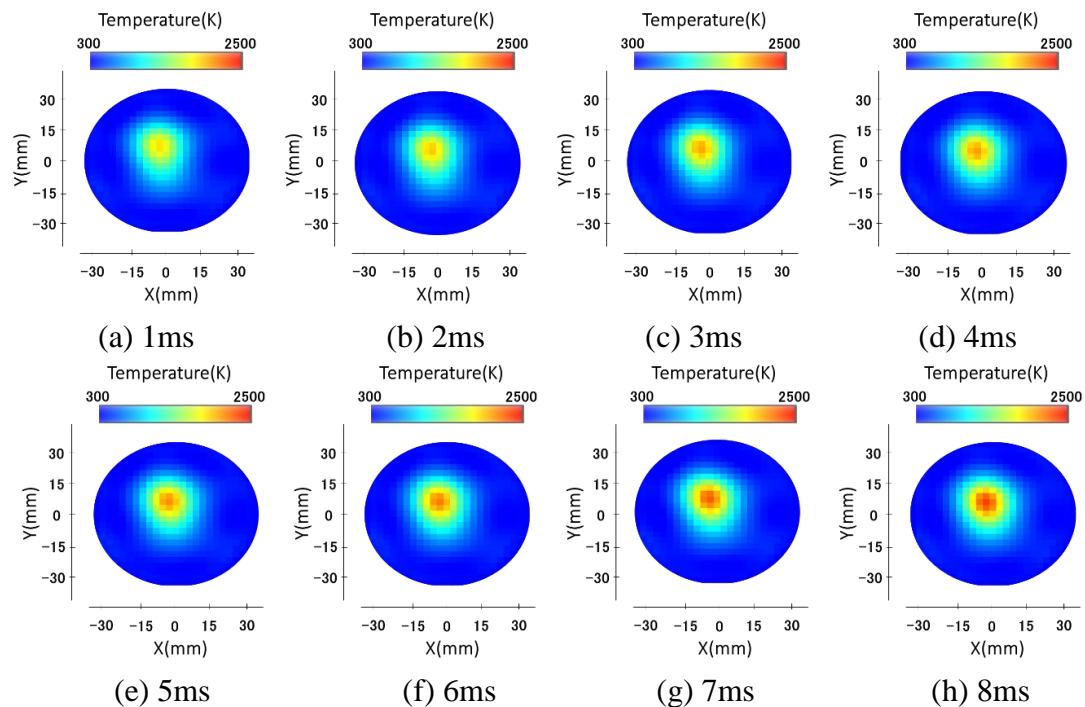
(a) 1ms   (b) 2ms   (c) 3ms   (d) 4ms

(e) 5ms   (f) 6ms   (g) 7ms   (h) 8ms

Figure 11 Time-series 2D temperature measurement results in pulverized coal flame.

5. Conclusions

Two dimensional temperature measurement characteristics of computed tomography-tunable diode laser absorption spectroscopy in the pulverized coal combustion field were investigated. The method is considerably new in combustion research, especially in pulverized coal combustion field. Based on the results of this study, the following conclusions are summarized.

1) The measurement accuracy of tunable diode laser absorption spectroscopy and the computed tomography reconstruction accuracy were evaluated first. The spectroscopic database was corrected by experimental results obtained using the measurement cell and the flat flame-type burner by tunable diode laser absorption spectroscopy to improve the temperature measurement accuracy of tunable diode laser absorption spectroscopy, which was compared to thermocouple results. The computed tomography reconstruction accuracy of 16-path configuration was evaluated using sum of squared difference and zero-mean normalized cross-correlation, which were good enough to be considered as almost the same patterns of assumed and reconstructed temperature distributions.

2) Two dimensional temperature measurement in pulverized coal combustion was measured using computed tomography-tunable diode laser absorption spectroscopy when introducing the pulverized coal to CH_4-Air flame. The time-series two dimensional temperature distributions of the pulverized coal flame were successfully measured by computed tomography-tunable diode laser absorption spectroscopy with 1 ms temporal resolution for online measurement.

3) The developed computed tomography-tunable diode laser absorption spectroscopy has a potential to be applicable to various flames even if with the particles, dusts and flame emissions, especially the pulverized coal combustion fields. The measurement results will be benefit for optimal operation control and combustion efficiency improvement.

Acknowledgement

References

[1] P.Y. Liu, J.J. Gao, H. Zhang, D.L. Zhang, Y.X. Wu, M. Zhang, J.F. Lu, Performance of the primary air concentrators on anthracite ignition and combustion in a 600 MW supercritical arch-fired boiler. Fuel Processing Technology 158 (2017) 172-179.

[2] H.H. Ma, L. Zhou, S.X. Ma, S.L. Yang, Y. Zhao, W. Zhang, J.W. Chew, Impact of multi-hole-wall air coupling with air-staged technology on H_2S evolution during pulverized coal combustion. Fuel Processing Technology 179 (2018) 277-284.

[3] Y. Deguchi, Industrial Applications of Laser Diagnostics. CRS Press: Taylor & Francis, New York, 2011.

[4] T. Kamimoto, Y. Deguchi, Y. Shisawa, Y. Kitauchi, Y. Eto, Development of fuel composition measurement technology using laser diagnostics. Applied Thermal Engineering 102 (2016) 596-603.

[5] Y. Deguchi, T. Kamimoto, Z.Z. Wang, J.J. Yan, J.P. Liu, H. Watanabe, R. Kurose, Applications of laser diagnostics to thermal power plants and engines. Applied Thermal Engineering 73 (2014) 1453-1464.

[6] R. Sur, K. Sun, J.B. Jeffries, J.G. Socha, R.K. Hanson, Scanned-wavelength-modulation-spectroscopy sensor for CO, CO_2, CH_4 and H_2O in a high-pressure engineering-scale transport-reactor coal gasifier. Fuel 150 (2015) 102-111.

[7] C.S. Goldenstein, C.A. Almodóvar, J.B. Jeffries, R.K. Hanson, C.M. Brophy, High-bandwidth scanned-wavelength-modulation spectroscopy sensors for temperature and H_2O in a rotating detonation engine. Measurement Science and Technology 25 (2014) 105104(11pp).

[8] M. Yamakage, K. Muta, Y. Deguchi, S. Fukada, T. Iwase, T. Yoshida, Development of direct and fast response exhaust gas measurement, SAE Technical Paper 2008-01-2758.

[9] G.B. Rieker, H. Li, X. Liu, J.T.C. Liu, J.B. Jeffries, R.K. Hanson, M.G. Allen, S.D. Wehe, P.A. Mulhall, H.S. Kindle, A. Kakuho, K.R. Sholes, T. Matsuura, S. Takatani, Rapid measurements of temperature and H_2O concentration in IC engines

with a spark plug-mounted diode laser sensor, Proceedings of the Combustion Institute 31 (2007) 3041-3049.

[10] H. McCann, P. Wright, K. Daun, Chemical species tomography, Industrial Tomography: Systems and Applications, Inc. Elsevier (2015) 135-174.

[11] W. Cai, C.F. Kaminski, A tomographic technique for the simultaneous imaging of temperature, chemical species, and pressure in reactive flows using absorption spectroscopy with frequency-agile lasers, Applied Physics Letters 104 (2015) 034101.

[12] P. Wright, N. Terzijaa, J.L. Davidsona, S. Garcia-Castillo, C. Garcia-Stewart, S. Pegrumb, S. Colbourneb, P. Turnerb, S.D. Crossleyc, T. Litt, S. Murrayc, K.B. Ozanyana, H. McCanna, High-speed chemical species tomography in a multi-cylinder automotive engine, Chemical Engineering Journal 158 (2010) 2-10.

[13] L. Ma, X. Li, S.T. Sanders, A.W. Caswell, S. Roy, D.H. Plemmons, J.R. Gord, 50-kHz-rate 2D imaging of temperature and H_2O concentration at the exhaust plane of a J85 engine using hyperspectral tomography, Optics Express 21 (2013) 1152-1162.

[14] S.A. Tsekenis, N. Tait, H. McCann, Spatially resolved and observer-free experimental quantification of spatial resolution in tomographic images, Review of Scientific Instruments 86 (2015) 035104.

[15] A. Seidel, S. Wagner, A. Dreizler, V. Ebert, Robust, spatially scanning, open-path TDLAS hygrometer using retro-reflective foils for fast tomographic 2-D water vapor concentration field measurements, Atmospheric Measurement Techniques 8 (2015) 2061-2068.

[16] C. Liu, L. Xu, Z. Cao, H. McCann, Reconstruction of axisymmetric temperature and gas concentration distributions by combining Fan-beam TDLAS with onion-peeling deconvolution, Transactions on Instrumentation and Measurement 63 (2014) 3067-3075.

[17] X. An, M.S. Brittelle, P.T. Lauzier, J.R. Gord, S. Roy, G. Chen, S.T. Sanders, 2015 Demonstration of temperature imaging by H_2O absorption spectroscopy using compressed sensing tomography, Applied Optics 54 (2015) 9190-9199.

[18] T. Kamimoto, Y. Deguchi, Y. Kiyota, High temperature field application of two dimensional temperature measurement technology using CT tunable laser absorption spectroscopy, Flow Measurement and Instrumentation 46 (2015) 51-57.

[19] T. Kamimoto, Y. Deguchi, D. Choi, J. Shim, Validation of the real-time 2D temperature measurement method using the CT tunable diode laser absorption spectroscopy, Heat Transfer Research 47 (2016) 193-202.

[20] X. An, T. Kraetschmer, K. Takami, S.T. Sanders, L. Ma, W. Cai, X. Li, S. Roy, J.R. Gord 2011 Validation of temperature imaging by H_2O absorption spectroscopy using hyperspectral tomography in controlled experiments, Applied Optics 50 (2011) A29-A37.

[21] L. Ma, W. Cai, Numerical investigation of hyperspectral tomography for simultaneous temperature and concentration imaging, Applied Optics 47 (2008) 3751-3759.

[22] M.G. Jeon, Y. Deguchi, T. Kamimoto, D.H. Doh, G.R. Cho, Performances of new reconstruction algorithms for CT-TDLAS (computer tomography-tunable diode laser absorption spectroscopy), Applied Thermal Engineering 115 (2017) 1148-1160

[23] Y. Deguchi, T. Kamimoto, Y. Kiyota, Time resolved 2D Concentration and temperature measurement using CT tunable laser absorption spectroscopy, Flow Measurement and Instrumentation 46 (2015) 312-318.

[24] T. Kamimoto, Y. Deguchi, N. Zhang, N. Nakao, T. Takagi, J.Z. Zhang, Real-time 2D concentration measurement of CH_4 in oscillating flames using CT tunable diode laser absorption spectroscopy, Journal of Applied Nonlinear Dynamics 4 (2015) 295-303.

[25] Y. Deguchi, D. Yasui, A. Adachi, Development of 2D temperature and concentration measurement method using tunable diode laser absorption spectroscopy, Journal of Mechanics Engineering and Automation, 2 (2012) 543-549.

[26] F. Wang, K.F. Cen, N. Li, J.B, Jeffries, Q.X. Huang, J.H. Yan, Y. Chi, Two-dimensional tomography for gas concentration and temperature distributions based

on tunable diode laser absorption spectroscopy, Measurement Science and Technology 21 (2010) 045301.

[27] V.L. Kasyutich, P.A. Martin, Towards a two-dimensional concentration and temperature laser absorption tomography sensor system, Applied Physics B: Lasers and Optics 102 (2011) 149-162.

[28] L.S. Rothman, I.E. Gordon, A. Barbe, D. ChrisBenner, P.F. Bernath, M. Birk, V. Boudon, L.R. Brown, A. Campargue, J.P. Champion, K. Chance, L. Coudert, V. Dana, V.M. Devi, S. Fally, J.M. Flaud, R.R. Gamache, A. Goldman, D. Jacquemart, I. Kleiner, N. Lacome, W.J. Lafferty, J.Y. Mandin, S.T. Massie, S.N. Mikhailenko, C.E. Miller, N. Moazzen-Ahmadi, O.V. Naumenko, A.V. Nikitin, J. Orphal, V.I. Perevalov, A. Perrin, A. Predoi-Cross, C.P. Rinsland, M. Rotger, M. Simeckova, M.A.H. Smith, K. Sung, S.A. Tashkun, J. Tennyson, R.A. Toth, A.C. Vandaele, J. VanderAuwera, The HITRAN2008 molecular spectroscopic database, Journal of Quantitative Spectroscopy & Radiative Transfer 110 (2009) 533-572.

Figure captions

Figure 1 CT configration with laser path and CT algorithm.

Figure 2 Experimental apparatus for evaluation of temperature measurement accuracy. (a) Measurement cell for low temperature range; (b) Flat flame burner for high temperature range.

Figure 3 Experimental system for 2D temperature measurement in pulverized coal combustion burner using CT-TDLAS. (a) CT-TDLAS experimental setup for a pulverized coal burner; (b) 16-path CT-TDLAS measurement cell.

Figure 4 Temperature distribution measured by thermocouple. (Average temperature in case 1: 2048K, case 2: 1864K, case 3: 1354K, case 4: 1265K, case 5: 1244K).

Figure 5 Theoretical and experimental absorption spectra of water vapor using uncorrected and corrected spectroscopic database in case 1. (a) Uncorrected (1388nm); (b) Corrected (1388nm); (c) Uncorrected (1343nm); (d) Corrected (1343nm).

Figure 6 Comparison of measured temperatures by TDLAS and thermocouple.

Figure 7 Comparison of temperature distributions calculated by 16-path CT-algorithm and assumed temperature in condition 1. (a)Assumed temperature; (b) CT reconstructed temperature; (c) Comparison at Y=0mm.

Figure 8 Comparison of temperature distributions calculated by 16-path CT-algorithm and assumed temperature in condition 2. (a)Assumed temperature; (b) CT reconstructed temperature; (c) Comparison at Y=0mm.

Figure 9 Comparison of temperature distributions at Y=0mm measured by 16-path CT-TDLAS and thermocouple in CH_4-Air flame.

Figure 10 2D temperature measurement results in CH_4-Air flame and pulverized coal flame using 16-path CT-TDLAS. (a) CH_4-Air flame; (b) pulverized coal flame.

Figure 11 Time-series 2D temperature measurement results in pulverized coal flame. (a) 1ms; (b) 2ms; (c) 3ms; (d) 4ms; (e) 5ms; (f) 6ms; (g) 7ms; (h) 8ms.